

## Analysis of Large Deformation Characteristics and Formability of PMMA

Min Jae Baek<sup>1,a</sup>, Yong Nam Kwon<sup>1,b</sup>, Daeho Jeong<sup>2,c</sup>, Ducksung Kim<sup>2,d</sup>,  
Yoo In Jeong<sup>2,e</sup>, and Hyunsung Choi<sup>1,f\*</sup>

<sup>1</sup>Korea Institute of Materials Science, Republic of Korea

<sup>2</sup>Korea Aerospace Industries, LTD, Korea, Republic of Korea

<sup>a</sup>qoralswo12@kims.re.kr, <sup>b</sup>kyn1740@kims.re.kr, <sup>c</sup>daeho.jeong@koreaaero.com,  
<sup>d</sup>ducksung.kim@koreaaero.com, <sup>e</sup>freud197@koreaaero.com, <sup>f</sup>h.choi@kims.re.kr

**Keywords:** PolyMethyl MethAcrylate (PMMA), Vacuum forming, High-temperature, Creep, Tensile, plastic deformation.

**Abstract.** Polymethylmethacrylate (PMMA) has been widely used for aircraft canopies and transparent structural components, and processed into various parts through vacuum forming. In this study, the effects of forming speed and deformation characteristics on thickness uniformity during high-temperature vacuum forming of PMMA were analyzed. First, creep tests and high-temperature tensile tests were conducted at the specimen level to quantitatively distinguish between creep deformation and plastic deformation. Creep tests were performed under constant temperature and load conditions, and strain was measured through Digital Image Correlation. For plastic deformation analysis, tensile tests at room temperature and elevated temperatures were carried out to compare yield strength and elongation changes. To analyze thickness uniformity during the forming process, rectangular-shaped parts were fabricated using vacuum forming under various conditions where temperature and forming speed are key variables. After forming, thickness uniformity and surface transparency of the products were measured. Additionally, internal structural changes according to forming speed and temperature conditions were analyzed, and a comprehensive evaluation of material stability was performed.

### Introduction

Poly(methyl methacrylate) (PMMA) is a synthetic polymer derived from methyl methacrylate monomers and designated by two IUPAC nomenclatures: poly[1-(methoxycarbonyl)-1-methyl ethylene] from a hydrocarbon perspective and poly(methyl 2-methyl-propenoate) from an ester perspective. PMMA was discovered in the early 1930s by British chemists Rowland Hill and John Crawford, and was first commercialized in 1934 by German chemist Otto Röhm. As an optically transparent thermoplastic, PMMA has been widely used as a glass substitute owing to its high impact strength, lightweight nature, shatter resistance, and excellent processability. Additionally, PMMA is characterized by outstanding weather resistance and scratch resistance. The methyl groups ( $-\text{CH}_3$ ) directly bonded to vinyl carbons in the PMMA polymer structure prevent polymer chains from packing densely in a crystalline fashion or rotating freely around C–C bonds. Consequently, PMMA is known as an amorphous thermoplastic. Furthermore, these methyl substituents elevate the glass transition temperature ( $T_g$ ), thereby increasing the stiffness of PMMA. The ester groups in PMMA impart high optical transparency and excellent optical properties. However, the polar interactions of these ester groups gradually weaken at elevated temperatures, resulting in creep deformation. The critical temperature at which this phenomenon occurs is the glass transition temperature ( $T_g$ ). The first major application of PMMA dates back to World War II, when it was adopted for aircraft windows and canopy components. This historical milestone demonstrated that PMMA's transparency, impact resistance, and lightweight characteristics could satisfy the stringent requirements of aviation applications. Today, PMMA continues to be extensively employed in transparent structural components of fighter aircraft and commercial airliners, being processed and manufactured into various shapes and functional parts through vacuum forming processes.

This study focuses on analyzing the effects of forming speed and deformation behavior on thickness uniformity in high-temperature vacuum forming processes of PMMA. Forming speed is a critical process variable directly related to production efficiency and economic viability. However, excessive forming speeds can induce localized deformation and thickness variation, while excessively slow speeds result in dramatically reduced production efficiency. Therefore, quantitative evaluation of PMMA's time-dependent behavior and irreversible deformation characteristics under various forming conditions is essential. In the PMMA vacuum forming process, forming temperature is the most critical variable determining process success. To accurately determine this optimal temperature, the glass transition temperature was measured in the present study. The glass transition temperature represents the temperature at which semi-crystalline or amorphous polymers transition from a glassy state to a rubbery state. At this critical temperature, the mechanical properties and behavior of the material undergo dramatic changes. Differential scanning calorimetry (DSC) was employed to precisely determine the glass transition temperature. Through DSC analysis, thermal property variations can be detected, and by tracking heat capacity changes in the glass transition region, the accurate  $T_g$  value can be determined. Repeated experiments confirmed that the glass transition temperature of PMMA exceeds  $110^{\circ}\text{C}$ [1–3]. To accurately characterize the forming behavior of PMMA, the viscoelastic behavior of the material and its deformation characteristics under prolonged loading were investigated in detail. Creep tests and elevated-temperature tensile tests were systematically conducted at the specimen level, and the resulting strain-time curves from each test condition were quantitatively compared and analyzed. Creep tests were conducted under constant temperature and load conditions. By continuously measuring strain evolution over time under a constant applied stress, creep curves were derived. This enabled investigation of the three characteristic creep regions and analysis of the strain rate progression in each stage. Notably, the creep characteristics observed in the elevated-temperature range similar to the forming temperature serve as important criteria for predicting the time-dependent large deformation behavior that occurs during actual vacuum forming processes[4–6]. To accurately characterize plastic deformation behavior, tensile tests were systematically conducted at both room temperature and elevated temperatures. This comprehensive analysis revealed detailed changes in key mechanical properties including yield strength, tensile strength, and elongation. The measurement results demonstrated a clear trend: as temperature increases, yield strength decreases while elongation increases[7–9]. This behavior directly correlates with increased material fluidity and enhanced formability at elevated temperatures, ultimately enabling the forming of complex geometries. To directly analyze thickness uniformity during the forming process, temperature and forming speed were established as primary process variables, and vacuum forming experiments were conducted across various parameter combinations[10–12]. Based on the experimental results, vacuum pressure, forming time, and the material temperature at the forming location were identified as the most critical factors for achieving uniform thickness in vacuum-formed products.

## Experiment

### Glass Transition Temperature

In the PMMA vacuum forming process, forming temperature is the most critical variable determining the success of the entire process. Forming temperature not only influences the workability of the material but also exerts a wide-ranging impact on the mechanical performance, dimensional stability, and surface quality of the final product. To accurately determine this optimal forming temperature, the glass transition temperature ( $T_g$ ) was measured in the present study. The glass transition temperature represents the temperature at which semi-crystalline or amorphous polymers transition from a glassy state to a rubbery state, and it is a fundamental yet most important physical parameter for understanding the structure and behavior of polymers. At the glass transition temperature, the molecular mobility and mechanical properties of the polymer undergo dramatic changes, which holds significant implications for the PMMA forming process. In this research, differential scanning calorimetry (DSC) was employed to measure the glass transition temperature. The DSC measurement

results, presented in the left graph, are attributed to the complex thermal behavior of PMMA and the subtle differences in specimen preparation conditions. However, through repeated experiments, it was confirmed that the glass transition temperature of PMMA exceeds 110 °C. Fig. 1

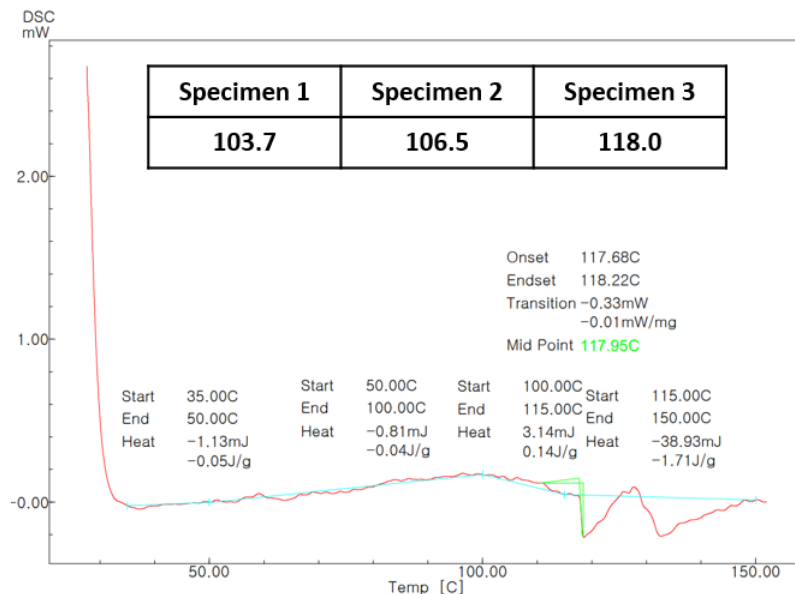


**Fig. 1.** Glass transition temperature measurement (differential scanning calorimetry)

### DIC-based strain measurement

Strain measurement was conducted using Digital Image Correlation (DIC). Fig. 2. Both high-temperature tensile tests and creep deformation exhibited large deformations, making it impossible to measure with conventional strain gauges. Therefore, we used DIC, a non-contact strain measurement technique. In this method, a speckle pattern is applied to the specimen surface, and specific points are tracked between two or more consecutive images using brightness distribution. The DIC measurements were conducted using the GOM 3D camera, with analysis parameters set to a facet size of 16 pixels and point distance of 13 pixels.

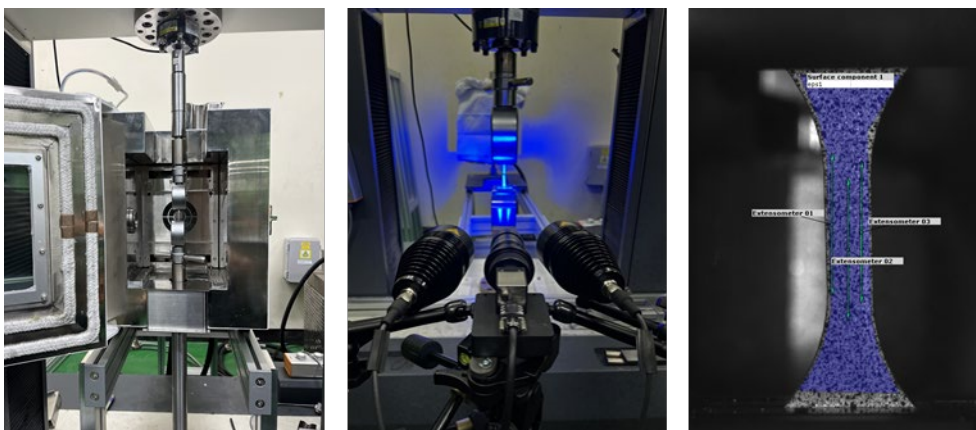
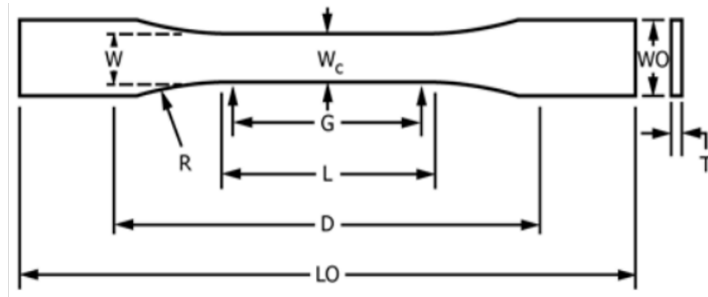


**Fig. 2.** Digital Image Correlation (DIC) for the strain measurement

### Strain rate-dependent uniaxial tensile test at room temperature

Room-temperature tensile tests were initially conducted to analyze basic material properties. The crosshead speeds for the tensile tests were 0.06 mm/min and 0.6 mm/min for the strain rate of 0.001/s and 0.01/s, respectively. To identify availability in subsequent elevated-temperature experiments, three different types of specimen geometry were machined according to ASTM D638-22. Fig. 3 shows Type 1, 2, and 3 specimens with gauge lengths of 165 mm, 246 mm, and 63.5 mm, respectively. These correspond to material specifications with thicknesses of  $\leq 7t$ ,  $\leq 14t$ , and  $\leq 4t$ , respectively. The

graph presented in Fig. 4a shows the tensile results for each specimen type. As can be seen, there was no significant variation in material properties depending on specimen geometry, especially for thickness. This indicates that the basic mechanical characteristics of PMMA are scarcely influenced by the geometric shape of the specimen, thus providing a reliable basis for selecting specific specimen geometries in subsequent elevated-temperature experiments. Fig. 4b presents the results of room-temperature tensile tests conducted at different strain rates. According to the results, there was no noticeable change in material properties with increasing strain rate at room temperature. This indicates that PMMA exhibits little strain-rate dependence at room temperature, demonstrating that the mechanical behavior of PMMA at room temperature is strain-rate independent.



Dimension (mm)	Type 1	Type 2	Type 3
W-width	13	19	3.18
L-Length	57	57	3.53
WO-Width	19	29	...
WO-Width	...	...	9.53
LO-Length	165	246	63.5
G-Gage length	50	50	7.62
D-Distance between grips	115	115	25.4
R-Radius of fillet	76	76	12.7
RO- Outer radius	...	...	...

Fig. 3. Specimen (unit : mm)

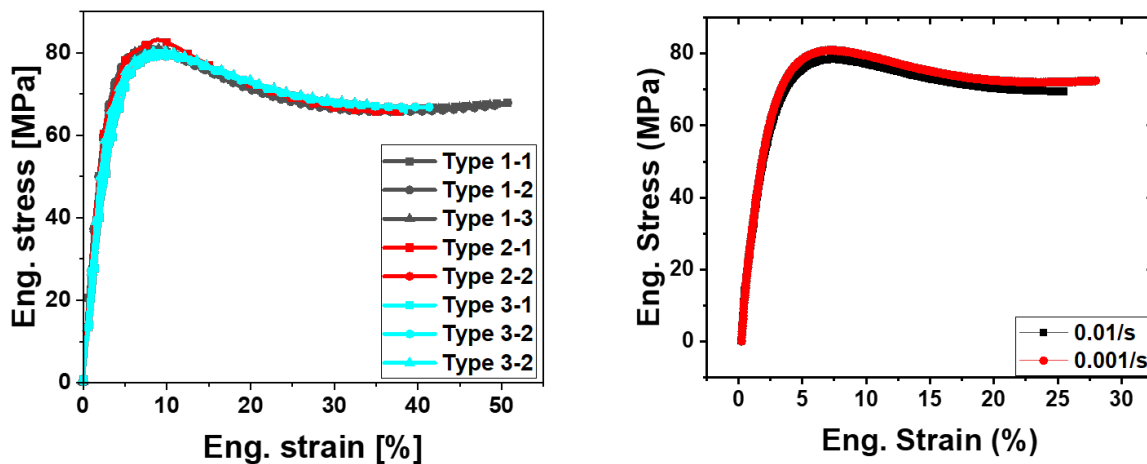
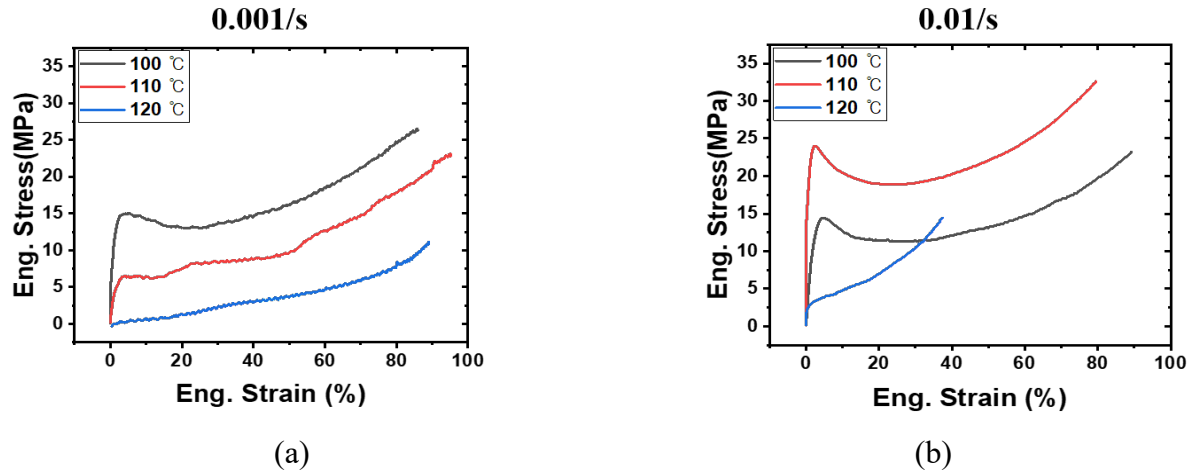


Fig. 4. (a) Tensile Test Results by Specimen Geometry and (b) Tensile Test Results at Different Strain Rates.

### High-temperature and strain rate-dependent tensile experiments

Considering the large deformations in elevated-temperature experiments, Type 1 specimen with a length of 165 mm and thickness of  $7t$  was employed. The experiments were conducted to analyze the high-temperature plastic behavior and strain rate-dependent behavior of PMMA, and to observe the high-temperature material behavior in the temperature range above the glass transition temperature.

Fig. 4 a shows the results at a strain rate of 0.001 /s, while Fig. 5 b presents the results at 0.01 /s. As evident from both results, the material exhibited softening behavior as temperature increased. Meanwhile, elongation increased with temperature; however, at 120 °C, which exceeds the glass transition temperature ( $T_g$ ), a decrease in elongation was observed. Additionally, the material stress at the glass transition temperature was extremely low.



**Fig.5.** High temperature tensile test results (a) HT Tensile Test Results at Strain Rate of 0.001/s and (b) HT Tensile Test Results at Strain Rate of 0.01/s

### Creep experiment

Creep tests were conducted to analyze material behavior in the forming process according to temperature, pressure, and time. Through these experiments, the creep deformation behavior of the material was observed under constant temperature, load, and time conditions. Test temperatures were conducted at 110 and 120 °C. The results presented in Fig. 6a were obtained at 110 °C (16 MPa, 17 MPa) and 120°C. At 110°C and 16 MPa, the secondary creep stage was confirmed. At 17 MPa, rapid strain increase occurred immediately after load application, followed by strain hardening and subsequent fracture. This demonstrates that under high-load conditions, the primary and secondary creep stages were shortened, resulting in rapid material deformation and fracture within a short period. Conversely, under low-load conditions, extended primary and secondary creep stages were observed. Additionally, at the test temperature of 120°C exceeding the glass transition temperature ( $T_g$ ), as shown in Fig. 6b expansion in the thickness direction of the gauge section was observed prior to load application, and localized contraction in the width direction caused specimen bending. This is presumed to be due to a restoration force generated as the material tends to return to its pre-stretched state. Through the creep tests, the importance of temperature as a process variable was confirmed, and the correlation between stress magnitude and forming time was also observed.

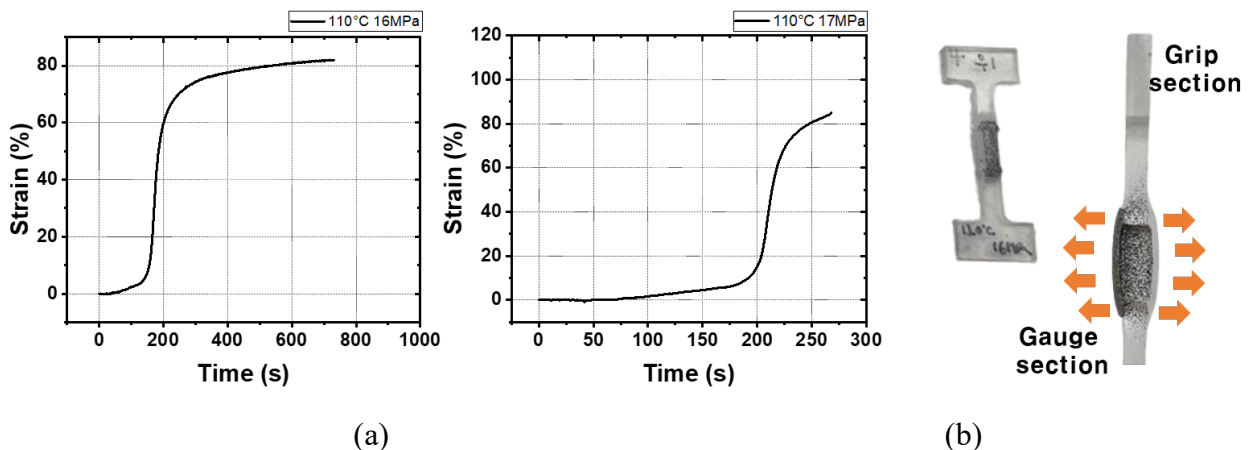


**Fig. 6.** Creep Test Results : (a) 110 °C, (b) 120 °C

### Lab scale Vacuum forming

Rectangular hot vacuum forming was carried out as shown in Fig. 7, consisting of an upper die, material, and lower die arranged sequentially, with the upper die applying clamping load. Vacuum sealing between the upper and lower dies was achieved using sealant tape and bagging film, and the process was designed to form a 100 mm × 100 mm shape. Specimens were initially processed at 130 mm × 130 mm with a thickness of 10t. The vacuum forming process parameters were temperatures of 100°C, 106°C, 110°C, and 120 °C; vacuum pressures of 0.3 bar, 0.5 bar, and 0.7 bar; and loads of 49, 59 and 98. The forming time was 12 hours, and thicknesses of 10 t were employed.

The experimental results at 100°C shown in Fig. 8 indicate that vacuum forming was not achieved due to detachment of the sealant tape. Additionally, excessive material thickness relative to the forming area hindered the success of vacuum forming. The results at 106°C presented in Fig. 8 demonstrate that under low vacuum pressure and high clamping load conditions, deformation was concentrated in the clamping area. Rapid cooling after load removal is presumed to have caused the increase in thickness. The results at 110°C shown in Fig. 8c can be compared to the drawing inflow amount. Non-uniform material inflow restriction was observed due to geometric constraints. The rectangular vacuum forming results at 120°C presented in Fig. 8d are as follows. The PMMA forming temperature exceeded the glass transition temperature ( $T_g$ ), and after forming, area shrinkage and increased thickness were observed. The presumed cause is considered to be related to the stretching manufacturing process. Cast billet material undergoes biaxial stretching to be manufactured into stretched acrylic, during which the area increases and thickness decreases, with improvements in strength, weather resistance, and impact resistance. Conversely, when the material temperature exceeds the glass transition temperature, a restoration force that drives the material to return to its cast billet state.

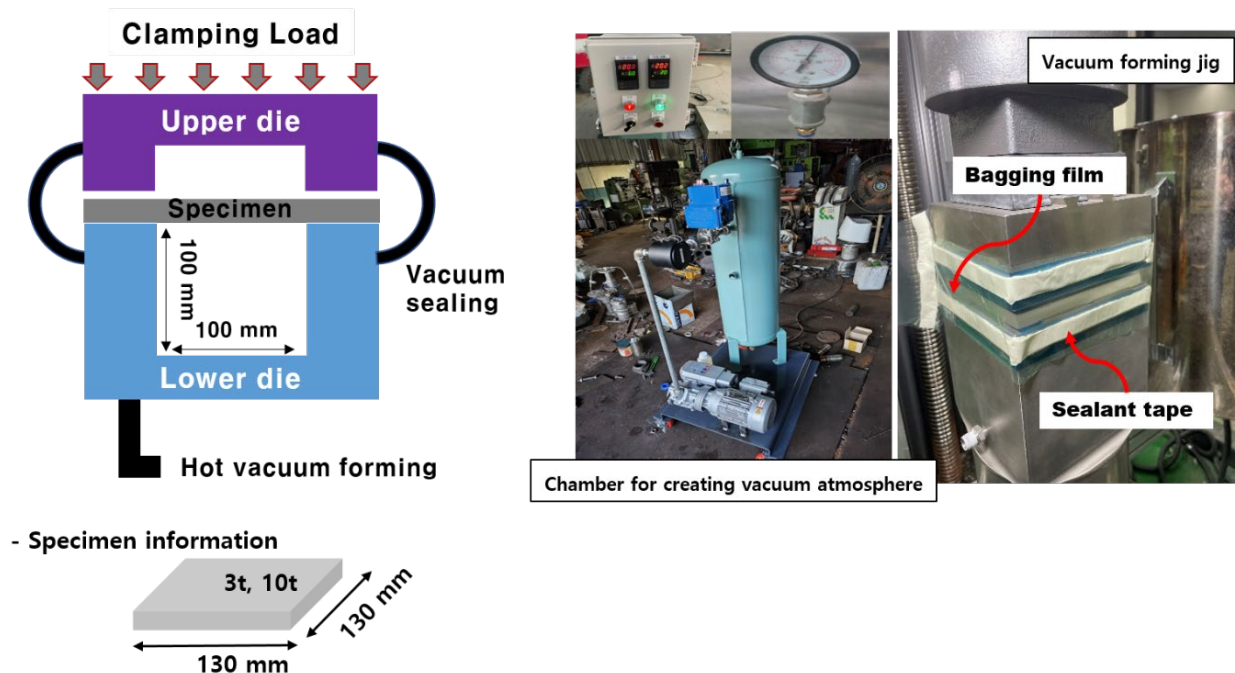
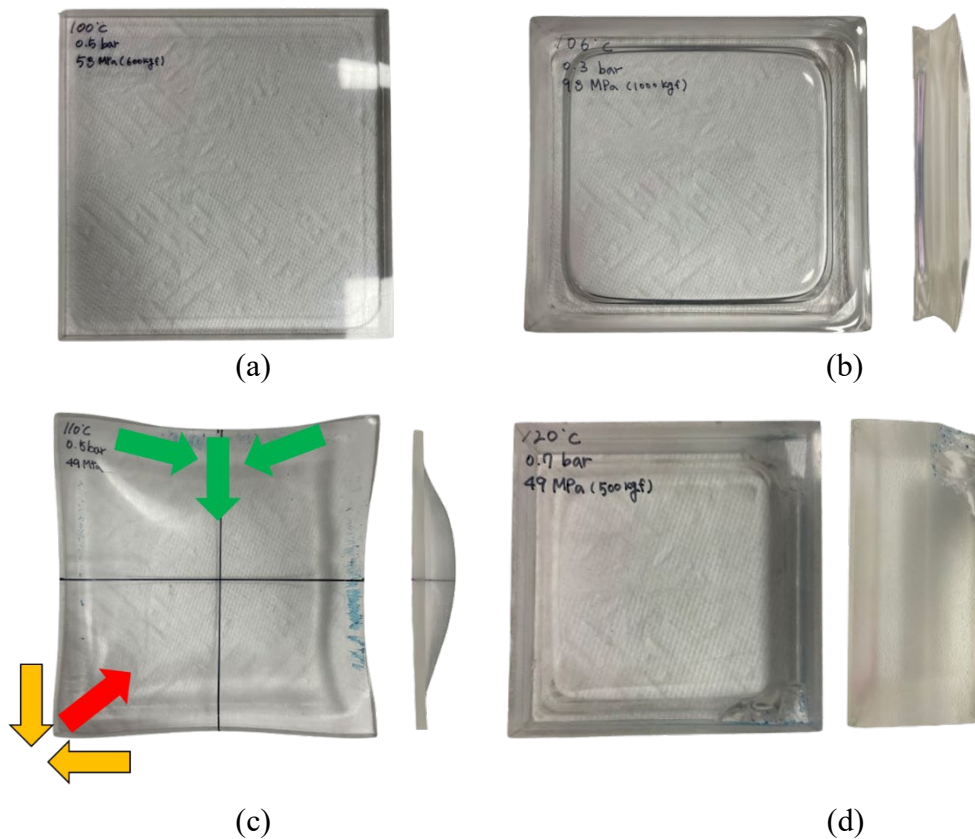


Fig.7. Rectangular Hot Vacuum Forming



**Fig. 8.** Lab scale Vacuum forming result: (a) 100°C, (b) 106 °C, (c) 110 °C, and (d) 120 °C.

### Summary

In the PMMA vacuum forming process, forming temperature is the most critical variable determining the success of the entire process and exerts a wide-ranging influence on the mechanical performance, dimensional stability, and surface quality of the final product. To accurately determine the forming temperature, the glass transition temperature ( $T_g$ ) was measured using differential scanning calorimetry (DSC), and it was confirmed that the  $T_g$  of PMMA exceeds 110°C. To measure the large deformations exhibited in elevated-temperature tensile tests and creep deformation, digital image correlation (DIC) was employed instead of contact-type gauges. In room-temperature tensile tests, basic material properties were analyzed using ASTM D638-22 compliant Type 1, 2, and 3 specimens (with gauge lengths of 165 mm, 246 mm, and 63.5 mm, respectively). At room temperature, no significant variation in material properties was observed depending on specimen geometry, and no characteristic changes with strain rate were detected, confirming that PMMA exhibits strain-rate independent characteristics at room temperature. In elevated-temperature experiments, Type 1 specimens with a length of 165 mm and thickness of 7 t were employed to analyze the high-temperature plastic behavior and strain rate-dependent behavior of PMMA. At both strain rates of 0.001 /s and 0.01 /s, softening behavior of the material was observed with increasing temperature, and elongation increased with temperature elevation but decreased at 120 °C (exceeding  $T_g$ ). In creep tests, the secondary creep stage was confirmed at 110°C with 16 MPa, while at the high-load condition of 17 MPa, the primary and secondary creep stages were shortened, resulting in fracture within a short period. Under low-load conditions, extended creep stages were observed, confirming that stress magnitude significantly influences forming time. In elevated-temperature creep tests at 120 °C, expansion in the thickness direction of the gauge section prior to load application and specimen bending due to localized contraction in the width direction were observed, which is presumed to result from a restoration force driving the material to return to its pre-stretched state. Rectangular hot vacuum forming experiments were composed of an upper die, material, and lower die, achieving vacuum sealing with sealant tape and bagging film to design the forming of a 100 mm

× 100 mm shape. The process variables were temperature (100°C, 106°C, 110°C, 120°C), vacuum pressure (0.3, 0.5, 0.7 bar), clamping load (49, 59, 98), and forming time (12 hours), with an initial thickness of 10 t. At 106 °C, under low vacuum pressure and high clamping load conditions, deformation was concentrated in the clamping area, and rapid cooling induced thickness increase. The experimental results at 110 °C revealed non-uniform material inflow restriction due to geometric constraints. At 120 °C, the forming temperature exceeded T<sub>g</sub>, resulting in material area shrinkage and thickness increase after forming. When material temperature exceeds T<sub>g</sub>, a restoration force is presumed to decrease the area and increase the thickness.

## References

- [1] Kusy, R. P., W. F. Simmons, and A. R. Greenberg. "Glass transition temperature of poly (methyl methacrylate) blends." *Polymer* 22.2 (1981): 268-270.
- [2] Ute, Koichi, Nobuo Miyatake, and Koichi Hatada. "Glass transition temperature and melting temperature of uniform isotactic and syndiotactic poly (methyl methacrylate) s from 13mer to 50mer." *Polymer* 36.7 (1995): 1415-1419.:
- [3] Porter, Crystal E., and Frank D. Blum. "Thermal characterization of PMMA thin films using modulated differential scanning calorimetry." *Macromolecules* 33.19 (2000): 7016-7020.
- [4] Kang, Suk-Choon. "Creep Characteristic of the Polymethyl Methacrylate (PMMA) at Stresses and Temperatures." *Journal of the Korean Society for Precision Engineering* 28.12 (2011): 1403-1410.
- [5] P.G. Clem, M. Rodriguez, J.A. Voigt and C.S. Ashley, U.S. Patent 6,231,666. (2001)
- [6] Triebel, C., and H. Münstedt. "Temperature dependence of rheological properties of poly (methyl methacrylate) filled with silica nanoparticles." *Polymer* 52.7 (2011): 1596-1602.
- [7] Abdel-Wahab, Adel A., Sabbah Ataya, and Vadim V. Silberschmidt. "Temperature-dependent mechanical behaviour of PMMA: Experimental analysis and modelling." *Polymer Testing* 58 (2017): 86-95.
- [8] Wu, Yiwen, et al. "Mechanical properties of constructional PMMA at elevated temperatures and postfire conditions." *Journal of Materials in Civil Engineering* 35.10 (2023): 04023377.
- [9] Van Loock, Frederik, and Norman A. Fleck. "Deformation and failure maps for PMMA in uniaxial tension." *Polymer* 148 (2018): 259-268.
- [10] O'Hanlon, John F. *A user's guide to vacuum technology*. John Wiley & Sons, 2003.
- [11] DEBELL, GEORGE W. "Use of Plastics and Allied Materials in Aircraft Construction." *Journal of the Aeronautical Sciences* 9.9 (1942): 341-349.
- [12] Raghuwanshi, R. K., and V. K. Verma. "Mechanical and thermal characterization of aero grade polymethyl methacrylate polymer used in aircraft canopy." *Int J Eng Adv Tech (IJEAT)* 3.5 (2014): 216-219.